Electron spin quantum beats in positively charged quantum dots: Nuclear field effects

L. Lombez, P.-F. Braun, X. Marie, P. Renucci, B. Urbaszek, and T. Amand*
Laboratoire de Physique et Chimie des Nano-Objets, UMR 5215, INSA-CNRS-UPS, 135 Avenue de Rangueil, 31077 Toulouse Cedex 4, France

O. Krebs and P. Voisin
Laboratoire de Photonique et Nanostructures, Route de Nozay, 91460 Marcoussis, France
(Received 22 December 2006; published 11 May 2007)

We have studied the electron spin coherence in an ensemble of positively charged InAs/GaAs quantum dots. In a transverse magnetic field, we show that two main contributions must be taken into account to explain the damping of the circular polarization oscillations. The first one is due to the nuclear field fluctuations from dot to dot experienced by the electron spin. The second one is due to the dispersion of the transverse electron Landé *g* factor, due to the inherent inhomogeneity of the system, and leads to a field-dependent contribution to the damping. We have developed a model taking into account both contributions, which is in good agreement with the experimental data. This enables us to extract the pure contribution to dephasing due to the nuclei.

DOI: 10.1103/PhysRevB.75.195314 PACS number(s): 73.21.La, 72.25.Fe, 72.25.Rb, 78.47.+p

I. INTRODUCTION

A single carrier spin in a single quantum dot represents a potential candidate for q-bit implementation in a solid-state environment, in view of applications in the fields of spintronics and quantum information processing.[1–4] Quantum dots (QDs) are indeed attractive with respect to the general criteria for quantum computers,[5] since long spin-relaxation times T_1 have been measured in neutral QDs, in the millisecond range for longitudinal magnetic field between 4 and 8 T.[6,7] This is made possible due to the inhibition of the random interactions leading to spin relaxation and decoherence in bulk[8] and quantum well semiconductor structures. However, one of the major difficulties in achieving quantum manipulations is decoherence due to interactions with an uncontrollable environment. Long spin decoherence times T_2 are, indeed, demanded in order to be able to achieve enough quantum manipulations during the spin lifetime T_1, and this requirement turns out to be the most stringent one. In principle, the dephasing rate due to spin-orbit coupling may reach values of the order of T_1.[9] Recent experiments have demonstrated a trend in this direction, where T_2 of the order of 1 μs could be measured at low temperature, allowing possible applications based on robust quantum coherence within an ensemble of dots.[10,11]

In quantum dots, two dephasing processes are still efficient and even enhanced by confinement: the exchange interaction between charges and the hyperfine interaction. The first one is responsible for various phenomena, such as, e.g., optically active exciton state splitting, neutral exciton quantum beats, and the appearance of negative circular polarization for negatively charged excitons under nonresonant excitation.[12–15] The second one, the hyperfine interaction of localized electrons with the QD nuclei, leads to very efficient spin dephasing.[16–19] This interaction effect has been observed previously in *p*-doped InAs/GaAs QDs for the ground state of the positively charged exciton (also called trion) X^+ by time-resolved photoluminescence (TRPL),[20] and more recently, in *n*-doped QDs for the resident electron using time-resolved Kerr pump-probe spectroscopy.[11,21] Three distinct time scales are relevant in describing the electron-nuclei spin system evolution:[16] the first time corresponds to the electron-spin precession around the frozen nuclear field fluctuations due to the QD nuclei (the typical dephasing time is of the order of 1 ns for GaAs QDs containing 10^5 nuclei); the second one is controlled by nuclear-spin precession in the hyperfine field of the localized electron (the typical time is of the order of 1 μs); and the last one is the nuclear-spin relaxation due to dipole-dipole interaction with nuclei in the vicinity of the QDs (the typical time is of the order of 100 μs). During the first two stages, the coherence of the electron–nuclear-spin system is preserved, while during the last one it is not, since the dipole-dipole interaction does not conserve the total nuclear spin. In Refs. 10 and 20, it is essentially the first dephasing stage which is observed, leading to an estimate of the electron-spin ensemble dephasing time T_2^* in the inhomogeneous nuclear field. The longer spin coherence times measured in Refs. 10 and 11 are based respectively on spin echo technique or mode locking of electron spin coherences to suppress the hyperfine induced dephasing, and are presumably limited by the nuclear-spin dephasing time.

In this work, we investigate the first stage of electron-spin dephasing in an ensemble of InAs/GaAs QDs in the presence of an in-plane magnetic field. To achieve this aim, we study the electron-spin coherence (ESC) in time-resolved photoluminescence spectroscopy of positively charged excitons X^+. Exciting QDs containing a single doping hole with an optical pulse results in the formation of a trion X^+, which, in its ground state, consists of a hole spin singlet in the highest valence states and a single electron spin in the lowest conduction orbital state:

$$\left|X^+, \pm\frac{1}{2}\right\rangle = \frac{1}{\sqrt{2}}\left(\left|\frac{3}{2},-\frac{3}{2}\right\rangle - \left|-\frac{3}{2},\frac{3}{2}\right\rangle\right) \otimes \left|\pm\frac{1}{2}\right\rangle, \quad (1)$$

where $|\pm\frac{3}{2}\rangle$ and $|\pm\frac{1}{2}\rangle$ represent respectively the projection of the heavy hole and conduction electron angular momentum on the quantification axis Oz, taken normal to the sample surface. Hence, the electron-hole exchange interaction,

which is efficient within neutral QD excitons,[14,22] is cancelled out.[20,23] The time- and polarization-resolved photoluminescence (TRPL) signal is thus a direct probe of the unpaired electron-spin dynamics during the radiative time. Note that in this approach, when exciting the dots within the wetting layer (WL), the holes lose their spin polarization before they are captured by the QDs (Refs. 15 and 24) due to efficient spin relaxation in the WL.[25] In addition, the spin coherence of localized holes that might be generated by the laser pulse, in a symmetrical way as for negatively charged dots,[21,26,27] will be cancelled out after the formation of the hole singlet in the trion ground state. Finally, the hyperfine interaction of the resident hole spin with the nuclei is negligible due to the *p* symmetry of the periodic part of the Bloch function.[28,29] Note also that, for *n*-doped QDs, the Kerr resonant pump-probe approach is very appropriate in studying long-term resident electron-spin evolution, particularly after the radiative recombination;[11,21] however, the response at short-time delay is more complex to analyze using this technique: both the dots with a photogenerated trion and the dots with a single carrier bearing an optically generated spin coherence contribute to the Kerr probe signal, leading to a complex interference pattern under transverse magnetic field [due to nonzero transverse *g* factor of the hole in QDs (Ref. 22)]. The TRPL experiment is then well adapted to make an accurate description of the unpaired electron-spin coherence of X^+ during the first step of its dephasing by nuclear spins. As we observe the average electron spin $\langle S_z(t)\rangle$ in an ensemble of dots, the decay of the oscillation amplitude can be described by a characteristic spin dephasing time T_2^*; in a classical view, this is the decoherence time of the spin ensemble during the precession around the applied transverse magnetic field, taking into account the different inhomogeneities of the sample.

We have developed a theoretical model to describe the quantum beats observed experimentally. We observe that two contributions participate in the spin dephasing: the first one is due to the nuclear field fluctuations. However, this contribution alone cannot explain the observed dephasing: the second contribution is due to static Landé *g*-factor fluctuations from dot to dot.[21,27] Finally, variations of QD doping level also have to be taken into account. By fitting our theoretical model to the experimental data, we can extract the contribution to the dephasing due to the hyperfine interaction alone. The hyperfine interaction is also responsible for the dephasing in a single quantum dot when averaging over a large number of nuclear field fluctuations. This is the case when the signal integration time is much larger than nuclear-spin relaxation time due to the dipole-dipole interaction.

II. SAMPLES AND EXPERIMENTAL SETUP

The samples used for this work consist of ten planes of self-assembled InAs QDs grown by Stranski-Krastanow method and separated by 30 nm of GaAs. A beryllium delta doping layer is located 15 nm below each wetting layer. Several samples have been investigated, with different nominal doping corresponding roughly to one hole per dot on average. We show here the results for two typical samples: sample 1 with a nominal doping of $N_A=5\times10^{10}$ cm^{-2} and sample 2 with a nominal doping of $N_A=15\times10^{10}$ cm^{-2}. The samples are mounted in a cryostat cooled at a temperature of 15 K. The experiment is performed in Voigt geometry, the external transverse magnetic field $\mathbf{B}=B_x\mathbf{e}_x$ being oriented along the *Ox* axis in the QD plane. The QDs are excited with 1.5 ps pulses from a mode-locked Ti-sapphire laser with a repetition rate of 80 MHz. Circularly polarized light ($\sigma+$) propagating along the growth axis *Oz* generates a coherent superposition of $|X^+,+1/2\rangle_x$ and $|X^+,-1/2\rangle_x$ trion eigenstates. The excitation beam is focused on a spot size of 100 μm diameter with an average power of 1 mW. We did not observe any change in the photoluminescence (PL) circular polarization dynamics for excitation powers up to 5 mW. The PL intensities copolarized (I^+) and counterpolarized (I^-) with the excitation laser are dispersed by a monochromator and then recorded using an S1 photocathode Hamamatsu streak camera with an overall time resolution of 30 ps. We measure the circular polarization degree of the photoluminescence $P_c=(I^+-I^-)/(I^++I^-)$, which corresponds directly to the electron average spin component $\langle S_z(t)\rangle=-P_c/2$ along *Oz*.[8]

III. RESULTS AND DISCUSSIONS

We present first the circular polarization (P_c) dynamics when increasing the magnetic field B_x up to 750 mT. The excitation energy ($E_{ex}=1.44$ eV) corresponds to the lowest states of the WL.[24] Under these excitation conditions we assume, consistently with previous experiments, that the electron maintains its spin orientation during the capture in QDs.[24] For sample 1, Fig. 1 presents the time evolution of the circular polarization $P_c(t)$ for three different magnetic fields B_x. At zero magnetic field, we find positive circular polarization (not shown) confirming that the QDs are *p* doped.[20] We recall that for neutral QDs, the anisotropic exchange interaction yields linearly polarized neutral exciton eigenstates, and under nonresonant excitation, the circular polarization value is lower than 3%.[23,30] For *n*-doped QDs, the eigenstates are circular, but the polarization rate is negative due to interplay of anisotropic exchange interaction and Pauli blocking.[15,19,24,31] Moreover, as we can observe luminescence under strictly resonant excitation (not shown here), we deduce that there are, on average, less than two holes per dot. We assume first that all the dots contain a single resident doping hole (this point will be discussed later). After relaxation, the optically excited and doping holes will finally form a singlet in the trion ground state, which recombines radiatively.

The oscillation period observed, corresponding to the X^+ ground-state Zeeman splitting ΔE, decreases when the magnetic field increases. The inset in Fig. 1 shows the linear dependence: $\Delta E=g_{\perp0}\mu_B B_x$. We can, thus, find the average transverse electron Landé *g* factor $|g_{\perp0}|\approx0.75\pm0.05$. Note that, as in quantum wells,[32–35] the electron effective Landé *g* factor is strongly anisotropic.[36]

From the curves $P_c(t)$ plotted in Fig. 1, we also see that despite the relatively high magnetic-field value, the ESC decays with a typical time T_2^* of about 300 ps. Increasing the

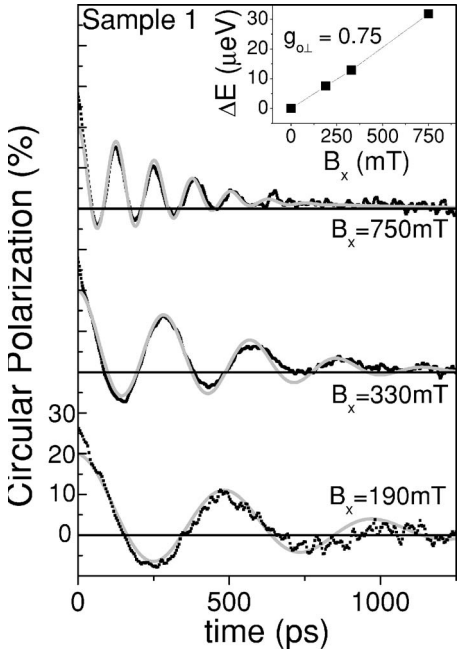

FIG. 1. Sample 1 ($N_A=5\times10^{10}$ cm^{-2}): time-resolved circular polarization decay of the X^+ trion under $\sigma+$ excitation for three different magnetic-field strengths B_x. Black dotted lines represent experimental curves; gray lines are theoretical curves (see text). Inset: Zeeman splitting as a function of B_x.

magnetic field also leads to an increase of the damping of the polarization oscillations. Furthermore, an unusual asymmetry of spin quantum beats is observed; the negative extrema of the circular polarization being smaller in absolute value than the positive ones, in contrast with what is commonly observed.[14,21,37,38] Comparing Figs. 1 and 2, we see that this asymmetry increases with the doping level of the structure.

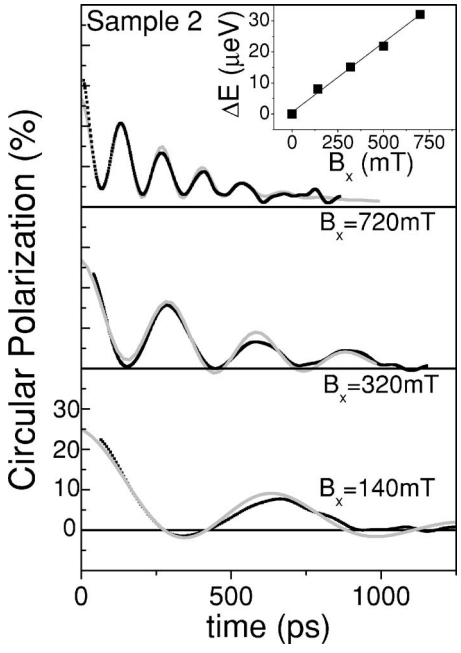

FIG. 2. Sample 2 ($N_A=15\times10^{10}$ cm^{-2}): same as Fig. 1 but increasing the doping level of the structure.

To explain these observations, we discuss first the role of the interaction of the trion with nuclei. Second, we will explain the dependence of the beat damping on B_x magnitude and the reason for the asymmetry. Finally, we will show the agreement between the experimental data and the different theoretical parameters used in this paper.

As the correlation time of the nuclear field is much longer than the X^+ trion lifetime,[20] we start from the model of the "frozen" configuration of nuclear spins.[16] In a first step, we only consider the electron-spin dephasing originating from the random distribution of the nuclear hyperfine field in the dots.

In order to determine the equation of motion of a spin in a dot, we adopt a similar approach as in Ref. 16. However, here, care has to be taken in order to take into account the g-factor anisotropy. It is thus more convenient to use the precession vector picture rather than the effective magnetic-field picture. The Hamiltonian of an electron in a dot is

$$H = H_N + H_Z, \tag{2}$$

$$H = v_0 \sum_i A_i |\Psi(\mathbf{R}_i)|^2 \hat{\mathbf{I}}_i \cdot \hat{\mathbf{S}} + (\mu_B \mathbf{g} \mathbf{B}_{ext}) \cdot \hat{\mathbf{S}}, \tag{3}$$

where the first term is the usual hyperfine contact Hamiltonian and the second is the Zeeman Hamiltonian. Here $\mathbf{g}$ is the electron g-factor tensor, $\hat{\mathbf{I}}_i$ and $\hat{\mathbf{S}}$ are writen in $\hbar$ units, and v_0 is the volume of the unit cell. The hyperfine interaction constants A_i are all of the order of 50 μeV considering two atoms per elementary cell.[39] We can thus write

$$H = \hbar \hat{\mathbf{\Omega}} \cdot \hat{\mathbf{S}} = \hbar (\hat{\mathbf{\Omega}}_N + \hat{\mathbf{\Omega}}_{ext}) \cdot \hat{\mathbf{S}}, \tag{4}$$

where $\hat{\mathbf{\Omega}}_N = v_0/\hbar \Sigma_i A_i |\Psi(\mathbf{R}_i)|^2 \hat{\mathbf{I}}_i$ is the precession vector operator and $\hat{\mathbf{\Omega}}_{ext} = \mu_B \mathbf{g} \mathbf{B}_{ext}/\hbar$. The quantum mechanical average of $\hat{\mathbf{\Omega}}_N$ on a given nuclear configuration is

$$\mathbf{\Omega}_N = \langle \hat{\mathbf{\Omega}}_N \rangle = \frac{v_0}{\hbar} \left\langle \sum_i A_i |\Psi(\mathbf{R}_i)|^2 \hat{\mathbf{I}}_i \right\rangle. \tag{5}$$

In the "frozen fluctuation" approach, $\mathbf{\Omega}_N$ evolves with time much slower than the electron average spin $\langle \hat{\mathbf{S}}(t) \rangle$. The electron sees a distribution of $\mathbf{\Omega}_N$, whose magnitude and direction are randomly distributed over the QD ensemble, described by an isotropic Gaussian probability density distribution function:

$$W(\mathbf{\Omega}_N) = \frac{1}{\pi^{3/2} \Delta_{\Omega_N}^3} \exp\left(- \frac{\mathbf{\Omega}_N^2}{\Delta_{\Omega_N}^2} \right), \tag{6}$$

where Δ_{Ω_N} represents the dispersion of the precession vector. The fluctuation of $\mathbf{\Omega}_N$ can be readily obtained assuming that the nuclear-spin directions are independent of each other:[16,20]

$$\Delta_{\Omega_N}^2 = \frac{2}{3} \langle\langle \mathbf{\Omega}_N^2 \rangle\rangle, \tag{7}$$

$$\Delta_{\Omega_N}^2 = \frac{1}{\hbar^2}\frac{n^2}{3N_L}\sum_j I^j(I^j+1)A_j^2, \tag{8}$$

where N_L is the number of nuclei interacting with the electron in a dot and n is the number of atoms in the lattice unit cell. The symbol $\langle\langle\cdots\rangle\rangle$ stands for averaging on the different nuclear field configurations. It is thus possible to define a characteristic dephasing time: $T_\Delta = \Delta_{\Omega_N}^{-1}$ (independent of the g-factor tensor). The equation of motion of an average spin $\langle\hat{\mathbf{S}}(t)\rangle$ in a fixed magnetic field in a QD is then given by

$$\langle\hat{\mathbf{S}}(t)\rangle = (\mathbf{S}_0\cdot\mathbf{n})\mathbf{n} + [\mathbf{S}_0 - (\mathbf{S}_0\cdot\mathbf{n})\mathbf{n}]\cos(\Omega t) + [\mathbf{S}_0 - (\mathbf{S}_0\cdot\mathbf{n})\mathbf{n}] \times \mathbf{n}\sin(\Omega t), \tag{9}$$

where $\mathbf{\Omega} = \mathbf{\Omega}_N + \mathbf{\Omega}_{ext}$, $\mathbf{n} = \mathbf{\Omega}/|\mathbf{\Omega}|$ is a unit vector, $\mathbf{\Omega}_N$ is the nuclear precession vector in a given QD as defined in Eq. (5), and $\mathbf{S}_0$ is the initial average electron spin.[16] $\Omega_{ext} = g_{eff}\mu_B B_{ext}/\hbar$ represents the contribution of the external field to the total precession vector $\mathbf{\Omega}$. In this expression, an effective Landé g factor has been introduced, which is defined by $g_{eff}^2 = g_\perp^2 \sin^2\eta + g_\parallel^2\cos^2\eta$, where $\eta = (\mathbf{e}_z, \mathbf{B}_{ext})$ is the angle of the external magnetic field with the Oz axis. The angle $\eta' = (\mathbf{e}_z, \mathbf{\Omega}_{ext})$ is given by $\eta' = \arctan\left(\frac{g_\perp}{g_\parallel}\tan\eta\right)$.

Expression (9) is then averaged over the QD ensemble, taking into account the Gaussian variations of $\mathbf{\Omega}_N$ characterized by Eq. (6).[16,20] The calculation is performed in the Appendix for an arbitrary orientation of the external magnetic field (the Ox axis is chosen in the plane defined by S_0 and B_{ext}). We assume that no dynamical polarization of the nuclei occurs, so that the ensemble average of $\mathbf{\Omega_N}$ is zero. For a pure transverse external field (Voigt configuration), this assumption is always valid, since no dynamical polarization of the nuclei (i.e., Overhauser effect) can occur.[40,44]

The average electron spin $\mathbf{S}(t) = \langle\langle\hat{\mathbf{S}}(t)\rangle\rangle$ can be expressed as the sum of two contributions $\mathbf{S}(t) = \mathbf{S}^\infty + \mathbf{S}_1(t)$, where S^∞ is time independent and $\mathbf{S}_1(t)$ contains the oscillating contribution which damps as t increases. The expressions $\mathbf{S}^\infty$ and $\mathbf{S}_1(t)$ are given respectively by the expressions (A9) and (A10).

For weak magnetic fields ($B_x < 200$ mT), taking $T_\Delta = 500$ ps as deduced from the measurement at zero magnetic field[20] leads to satisfactory fits of the experimental data. However, for larger magnetic fields, we will see below that the contribution of the nuclear field fluctuations is not sufficient to explain the observed damping (see Fig. 5). Moreover, the dephasing time T_Δ is field dependent, which contradicts the fact that, under transverse magnetic field, the nuclear field fluctuations are, in principle, insensitive to the applied magnetic field.

In fact, the magnetic-field-dependent damping arises from variations of the electron g factor over the QD ensemble, leading to a spreading of the Larmor frequencies with increasing B_x.[21,27] For instance, the origin of this inhomogeneity could come from the different dot sizes or chemical repartition of In in the QDs. This contribution is the second source of spin dephasing for an ensemble of quantum dots. Under the reasonable assumption that the nuclear field and g-factor fluctuations are uncorrelated, we have included the variations of the latter in the model of Merkulov *et al.*[16] For an arbitrary magnetic-field orientation, we did the simplifying assumption that the transverse and longitudinal fluctuations ($\delta g_\perp$ and $\delta g_\parallel$, respectively) are strongly correlated, according to

$$\frac{\delta g_\perp}{\delta g_\parallel} \approx \frac{g_\perp}{g_\parallel} \approx \frac{g_{\perp 0}}{g_{\parallel 0}}, \tag{10}$$

where $g_{\perp(\parallel)0}$ is the average $g_{\perp(\parallel)}$ value. Under this assumption, only the amplitude of Ω_{ext} fluctuates from dot to dot, but not its direction, which is given by the angle $\eta' = \arctan\left(\frac{g_{\perp 0}}{g_{\parallel 0}}\tan\eta\right)$. This approach yields exact results for purely transverse or purely longitudinal magnetic fields. For oblique fields, it gives some interpolation between the two cases. The fluctuations of the precession vector due to external magnetic field are now given by the Gaussian distribution:

$$W(\Omega_{ext}) = \frac{1}{\sqrt{2\pi}\Delta_\Omega}\exp\left(-\frac{(\Omega_{ext}-\Omega_0)^2}{2\Delta_\Omega^2}\right), \tag{11}$$

where $\mathbf{\Omega}_{ext} = \Omega_{ext}\mathbf{e}'_\eta$, $\Omega_0 = \mu_B(g_{\perp 0}^2\sin^2\eta + g_{\parallel 0}^2\cos^2\eta)^{1/2}B_{ext}$, and Δ_Ω, defined by $\Delta_\Omega^2 = \Delta g_\perp^2\sin^2\eta + \Delta g_\parallel^2\cos^2\eta$, characterizes the fluctuation of the precession vector length. Note that this corresponds to a Gaussian probability distribution characterized by the parameter $\Delta_{g_{eff}}$ and the average value $g_{eff,0}$.

Then expression (9) can be averaged by taking both Gaussian variations for B_N and $g_\perp$. The new equations for $\mathbf{S}^\infty$ and $\mathbf{S}_1(t)$ are now given respectively by the expression (A9) taken for $g_{eff,0}$ and Eq. (A22), from which the time-resolved circular polarization can be deduced.

Let us now explain the different effects of the nuclear field fluctuations and the g-factor fluctuations. The obtained theoretical curves derived from the model developed in the Appendix are shown in Fig. 3 for $B_x = 150$ mT and in Fig. 4 for $B_x = 750$ mT. In Figs. 3(a) and 4(a), the nuclear field fluctuations are kept constant ($T_\Delta = 500$ ps), while the g-factor fluctuations increase. In Figs. 3(b) and 4(b), $\Delta_g/g_{0\perp}$ is kept constant at 0.07 while the nuclear fluctuations increase. From the comparison of both figures, it is clearly seen that, at weak transverse magnetic field, the damping of the oscillations is mostly determined by the nuclear field fluctuations, while both contributions are necessary under larger magnetic field using realistic sets of parameters.

Note that the curve in Fig. 3(a) for g-factor fluctuations $\Delta_g/g_{\perp 0} = 0$ allows us to extract the contribution of the hyperfine interaction [the equation of the spin quantum beats is given by the expressions (A9) plus (A10)]. We clearly see that the nuclear field fluctuations lead to a first contribution to damping of the P_c oscillations even for the strongest B_x applied. The transverse magnetic field B_x is responsible for a large amplitude of spin quantum beats and yields a precise measurement of the spin decoherence time T_2^*. The characteristic dephasing time appearing in the model at zero magnetic field is $T_\Delta = \Delta_{\Omega_N}^{-1}$, which here has a typical value of $T_\Delta = 500$ ps. The characteristic time for the decay of the oscillation amplitude is $2T_\Delta$ [see Eq. (A10)].

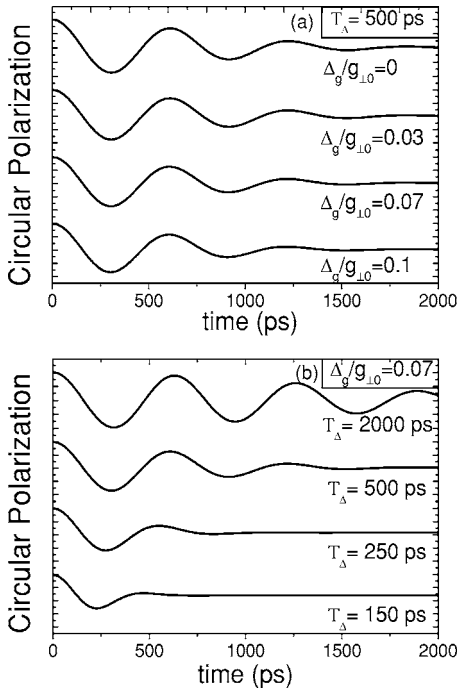

FIG. 3. Theoretical curves from the model developed in the Appendix, showing the spin quantum beats in a weak transverse magnetic field (B_x=150 mT) when the amplitude of the g factor and the nuclear field fluctuations vary. (a) Fixed nuclear field fluctuations (T_Δ=500 ps) and increasing g fluctuations. (b) Fixed g-factor fluctuations ($\Delta_g/g_{\perp 0}$=0.07) and increasing nuclear field fluctuations (i.e., decreasing the parameter T_Δ).

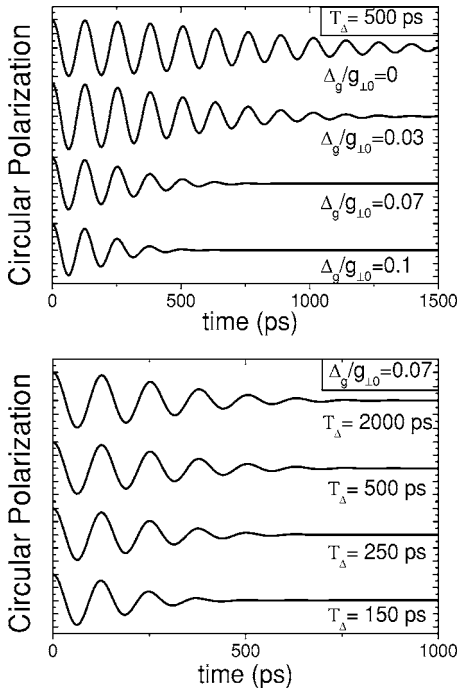

FIG. 4. Same as Fig. 3 but for a stronger transverse magnetic field (B_x=750 mT).

The variations of $P_c(t)$ according to the model including the g-factor fluctuations are displayed in Fig. 5 for $\Delta_g/g_{\perp 0}$ =0.07 and $\Delta_g/g_{\perp 0}$=0, for comparison. We see that, as expected, the g-factor fluctuations lead to an increase of the dephasing. The new characteristic dephasing time T_2^* for an ensemble of dots is now given by

$$T_2^* = \frac{T_\Delta}{\left[1 + 2\left(\frac{\Delta_{g_{eff}}}{g_{eff,0}}\frac{B}{\Delta_B}\right)^2\right]^{1/2}}, \tag{12}$$

where $\Delta_B = \hbar/g_{eff}\mu_B T_\Delta$. The variations of T_2^*/T_Δ with the magnetic field are displayed in Fig. 6 (bold line). When the magnetic field is much stronger than the nuclear field fluctuations ($B \gg \Delta_B \cdot g_{eff,0}/\Delta_{g_{eff}}$), these variations can be approximated by

$$T_2^* = \frac{1}{\sqrt{2}}\frac{g_{eff,0}}{\Delta_g}\frac{\Delta_B}{B}T_\Delta. \tag{13}$$

The corresponding dotted line in Fig. 6, which is the expression taken in Ref. 21, is given for comparison.

At this stage, the model correctly describes the period and the damping of the electron-spin quantum beats. For transverse magnetic field comparable to the nuclear field fluctuation, the beats are nonsymmetrical with respect to P_c=0. However, in the investigated range, B_x is stronger than Δ_B, which results in symmetrical $P_c(t)$ oscillations. Thus, the observed asymmetry remains to be explained.

We believe that the origin of this asymmetry lies in the QD charge fluctuations. Besides dots doped with a single resident hole, some are neutral and some contain two resident holes, so that neutral excitons (X^0) and doubly charged excitons (X^{2+}) are detected. The anisotropic exchange interaction (AEI) between electron and hole in X^0 and X^{2+} would lead, in principle, to beats of $P_c(t)$ for these QDs even for B_x=0.[14,15] However, the latter quickly damps due to the strong dispersion of the exchange energy from dot to dot.[22,41–43] For X^0 and X^{2+}, the spin-polarization decay can be

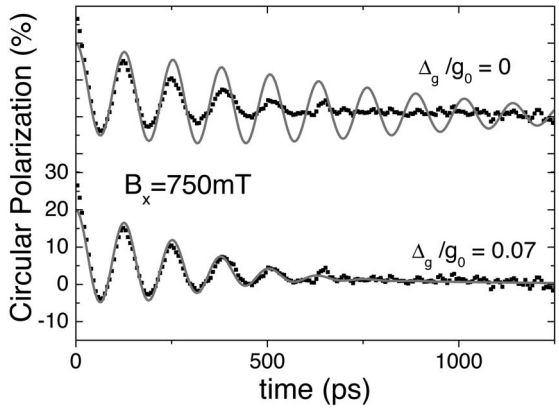

FIG. 5. Sample 1: comparison of experimental (dotted line) and theoretical curves of time-resolved circular polarization for B_x =750 mT. The theoretical curves (gray line) is given with ($\Delta_g/g_{0\perp}$=0.07) or without ($\Delta_g/g_{0\perp}$=0) g-factor fluctuations. Here T_Δ=500 ps and T_x^*=400 ps (see text).

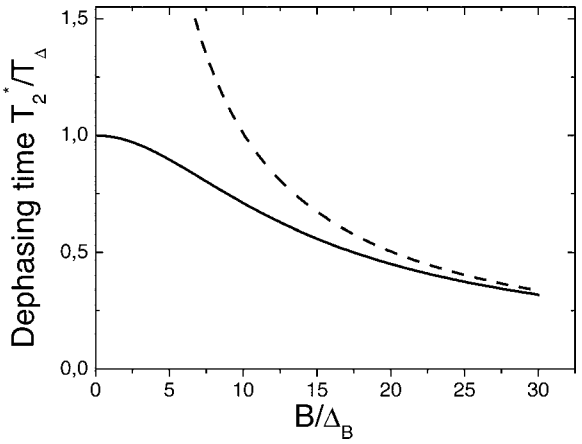

FIG. 6. Dephasing time as function of the relative magnetic field. The dotted line shows the exponential model used in Ref. 21. The bold line represents our calculations [see Eq. (12)].

described by $\mathbf{S}(t)=S_0e^{-t/T_x^*}$, where T_x^* is an ensemble inhomogeneous dephasing time. This expression is valid provided that the dispersion of the AEI energy is of the same order of magnitude as its average value. Defining α as the relative number of dots with charge state other than 1, the time evolution of the circular polarization is given by $P_c(t)=-2S_0[(1-\alpha)S(t)/S_0+\alpha e^{-t/T_x^*}]$.[45] The theoretical curves of $P_c(t)$ in Fig. 5 (gray lines) are displayed using the parameters $T_\Delta=500$ ps, $\alpha=0.4$ and $T_x^*=400$ ps, with $(\Delta_g/g_{0\perp}=0.07)$ and without $(\Delta_g/g_{0\perp}=0)$ g-factor fluctuations and are compared to the experimental curve (dotted line).

To summarize, the only adjustable parameters of the model are $\Delta_g/g_{\perp 0}$, T_x^*, and the weight α of QDs with zero or two holes (depending on the doping distribution), all independent of the magnetic field. The nuclear field fluctuations in the QD ensemble are determined from a fit of the circular polarization without magnetic field[20] and the average transverse g factor $g_{\perp 0}$ from the period of the oscillations (see Fig. 1). Note that $\Delta_g/g_{\perp 0}=0.07$ is consistent with previous studies.[36]

The curves on Figs. 1 and 2 are fitted using a unique set of parameters $\Delta_g/g_{\perp 0}$ and T_x^*, changing only the magnetic field. The parameter α takes into account that sample 2 ($N_A=15\times10^{10}$ cm^{-2}) is doped more than sample 1 ($N_A=5\times10^{10}$ cm^{-2}). We take $\alpha=0.4$ for sample 1 and 0.6 for sample 2. We observe good agreement between theory and experiment for several applied transverse magnetic fields.

In conclusion, we have developed a model to describe electron-spin dynamics in an ensemble of p-doped QDs under transverse magnetic fields. We have shown that (i) the hyperfine interaction, (ii) g-factor fluctuations from dot to dot, and (iii) QD charge variations have to be taken into account to explain the time evolution of the emitted circular polarization P_c. The experiments presented here demonstrate the key role played by the nuclear field fluctuations on the electron-spin coherence dynamics in QDs and we found a dephasing time of about 1 ns for this contribution. Note that in single QD experiments, only the contribution due to the interaction with the nuclei should be observed.

ACKNOWLEDGMENTS

We are grateful to K. V. Kavokin for fruitful discussions and to A. E. Zhukov, V. M. Ustinov, and V. K. Kalevich for sample growth and preparation. We thank MOMES ANR and FSE for financial support. X.M. acknowledges the support from Institut Universitaire de France.

APPENDIX: THEORETICAL MODEL

We first take into account only the fluctuations of the hyperfine field represented by Eq. (6). The calculation is performed in such an $(OXYZ)$ frame that the precession vector $\mathbf{\Omega}_{ext}$ is along the OZ axis $[\eta'=(\mathbf{e}_z,\mathbf{e}_Z)]$ and the initial electron-spin axis $\mathbf{S}(0)$ is in the (XOZ) plane, i.e., OX belongs to the $(\mathbf{S}(0),\mathbf{\Omega}_{ext})$ plane.

Averaging Eq. (9) of the spin motion, we can find the evolution of the mean spin as a function of time; we obtain

$$\mathbf{S}(t)=\mathbf{S}^\infty+\mathbf{S}_1(t). \tag{A1}$$

The first contribution is time independent. It represents the asymptotic limit for $\mathbf{S}(t)$ when $t\to\infty$. The different values of $\mathbf{S}(t)$ in the $(OXYZ)$ frame are

$$S_X^\infty=\frac{S_{0X}}{2\beta^2}\left(1-\frac{1}{\sqrt{\pi}}\int_{-\infty}^{\infty}e^{-(z^2+\beta^2)}\frac{e^{2\beta z}-1}{2\beta z}dz\right),$$

$$S_Y^\infty=0,$$

$$S_Z^\infty=\frac{S_{0Z}}{\beta^2}\left(\beta^2-1+\frac{1}{\sqrt{\pi}}\int_{-\infty}^{\infty}e^{-(z^2+\beta^2)}\frac{e^{2\beta z}-1}{2\beta z}dz\right). \tag{A2}$$

We use in this appendix $\beta=\frac{\Omega_{ext}}{\Delta_{\Omega_N}}$, $z=\frac{\Omega}{\Delta_{\Omega_N}}$, and $\tau=\frac{t}{T_\Delta}$ as reduced parameters in units of the nuclear contribution to the precession vector fluctuation. The parameter z is taken algebraically and we recall that $\mathbf{\Omega}=\mathbf{\Omega}_{ext}+\mathbf{\Omega}_N=\Omega\cdot\mathbf{n}$.

Note that the relation

$$2\frac{S_X^\infty}{S_{0X}}+\frac{S_Z^\infty}{S_{0Z}}=1 \tag{A3}$$

is fulfilled (see Ref. 16) whatever the value of β is.

The second contribution contains the oscillating contributions which damp with a typical time $2T_\Delta$. We define the following integrals:

$$I(\beta,\tau)=\frac{e^{\tau^2/4-\beta^2}}{\sqrt{\pi}}\int_{-\infty}^{\infty}e^{-z^2}\frac{e^{2\beta z}-1}{2\beta z}\cos(z\tau)dz, \tag{A4}$$

$$I(\beta,\tau)=\frac{1}{2\beta}\left[\cos(\beta\tau)I_2(\beta,\tau)+\frac{\tau}{2}\sin(\beta\tau)I_1(\beta,\tau)-e^{-\beta^2}I_2(0,\tau)\right] \tag{A5}$$

using the following auxilliary integrals:

$$I_1(\beta,\tau)=\frac{1}{\sqrt{\pi}}\int_{-\infty}^{\infty}\frac{e^{-(z-\beta)^2}}{z^2+\tau^2/4}dz, \tag{A6}$$

$$I_2(\beta,\tau)=\frac{1}{\sqrt{\pi}}\int_{-\infty}^{\infty}\frac{ze^{-(z-\beta)^2}}{z^2+\tau^2/4}dz. \tag{A7}$$

We can thus rewrite the different components of $\mathbf{S}^{\infty}$ as

$$S_X^{\infty}=\frac{S_{0X}}{2\beta^2}[1-I(\beta,0)],$$

$$S_Y^{\infty}=0,$$

$$S_Z^{\infty}=\frac{S_{0Z}}{\beta^2}[\beta^2-1+I(\beta,0)], \tag{A8}$$

and thus

$$S_X^{\infty}=\frac{S_{0X}}{2\beta^2}\left\{1-\frac{1}{2\beta}[I_2(\beta,0)-e^{-\beta^2}I_2(0,0)]\right\},$$

$$S_Y^{\infty}=0,$$

$$S_Z^{\infty}=\frac{S_{0Z}}{\beta^2}\left\{\beta^2-1+\frac{1}{2\beta}[I_2(\beta,0)-e^{-\beta^2}I_2(0,0)]\right\}. \tag{A9}$$

The oscillating contributions $\mathbf{S}_1(t)$ are given by the following expressions:

$$S_{1X}(t)=S_{0X}e^{-\tau^2/4}\left\{\left(1-\frac{1}{2\beta^2}\right)\cos(\beta\tau)-\frac{\tau}{2\beta}\sin(\beta\tau)+\frac{1}{2\beta^2}I(\beta,\tau)\right\},$$

$$S_{1Y}(t)=-S_{0X}e^{-\tau^2/4}\left\{\left(1-\frac{1}{2\beta^2}\right)\sin(\beta\tau)+\frac{\tau}{2\beta}\cos(\beta\tau)\right\},$$

$$S_{1Z}(t)=\frac{S_{0Z}}{\beta^2}e^{-\tau^2/4}\{\cos\beta\tau-I(\beta,\tau)\}. \tag{A10}$$

Note that the following relation holds:

$$\frac{d}{dt}\left[\frac{2S_{1X}(t)}{S_{0X}}+\frac{S_{1Z}(t)}{S_{0Z}}\right]=2\Omega_{ext}\frac{S_{1Y}(t)}{S_{0X}}. \tag{A11}$$

For the integral $I(\beta,0)$, the series expansion can be given as

$$I(\beta,0)=e^{-\beta^2}\sum_{p=0}^{\infty}\frac{\beta^{2p}}{p!(2p+1)}. \tag{A12}$$

From this expression, we can calculate $I(0,0)$ and find the same limit as in Ref. 16:

$$S_X^{\infty}\approx\frac{1}{3}S_{0X},\quad S_Y^{\infty}=0,\quad S_Z^{\infty}\approx\frac{1}{3}S_{0Z}. \tag{A13}$$

For small magnetic field ($\beta\ll 1$), the general expression of $\mathbf{S}(t)$ is, up to second order with respect to β,

$$S_X(t)=\frac{S_{0X}}{3}\left\{1+2e^{-\tau^2/4}\left(1-\frac{\tau^2}{2}\right)\right\}+O(\beta^2),$$

$$S_Y(t)=0,$$

$$S_Z(t)=\frac{S_{0Z}}{3}\left\{1+2e^{-\tau^2/4}\left(1-\frac{\tau^2}{2}\right)\right\}+O(\beta^2). \tag{A14}$$

Another limiting case is found at high magnetic field ($\beta\gg 1$). The expression for $\mathbf{S}^{\infty}$ is

$$S_X^{\infty}\approx 0,\quad S_Y^{\infty}\approx 0,\quad S_Z^{\infty}\approx S_{0Z},$$

and the expression for $\mathbf{S}_1(t)$ is

$$S_{1X}(t)=S_{0X}e^{-\tau^2/4}\cos(\beta\tau),$$

$$S_{1Y}(t)=-S_{0Y}e^{-\tau^2/4}\sin(\beta\tau),$$

$$S_{1Z}(t)=0, \tag{A15}$$

and finally, the expression for $\mathbf{S}(t)$:

$$S_X(t)=S_{0X}e^{-\tau^2/4}\cos(\beta\tau),$$

$$S_Y(t)=-S_{0Y}e^{-\tau^2/4}\sin(\beta\tau),$$

$$S_Z(t)=S_{0Z}. \tag{A16}$$

Note that, at long-time delay, we have $\mathbf{S}_1(t)\to 0$ and $\mathbf{S}(t)\to S^{\infty}$ when $\tau\to\infty$.

Let us now discuss the averaging of Eqs. (A9) and (A10) if we take into account the g-factor fluctuations. We introduce the effective g factor by the expression

$$\frac{g_{eff}\mu_B B_{ext}}{\hbar}=\Omega_{ext}, \tag{A17}$$

where

$$g_{eff}^2=g_{\perp}^2\sin^2\eta+g_{\parallel}^2\cos^2\eta \tag{A18}$$

and $\eta=(\mathbf{e}_z,\mathbf{B}_{ext})$.

The g-factor fluctuations lead to Ω_{ext} variations given by expression (11) where

$$\Delta_{\Omega}=\frac{\Delta_{g_{eff}}\mu_B B_{ext}}{\hbar}. \tag{A19}$$

Using the expression $\beta=\Omega_{ext}/\Delta_{\Omega_N}$, we obtain

$$\Delta_{\beta}=\frac{\Delta_{g_{eff}}\mu_B B_{ext}}{\hbar\Delta_{\Omega_N}}. \tag{A20}$$

We assume in our model that

$$\frac{\Delta_{\beta}}{\beta}=\frac{\Delta_{g_{eff}}}{g_{eff}}\ll 1. \tag{A21}$$

Moreover, if $\beta\geqslant\pi$ (i.e., $B_{ext}\gg h/2g_{eff}\mu_B T_{\Delta}$), the envelope of the average spin oscillations decays much slower than the period of these oscillations. It follows that, in order to average $\mathbf{S}(t)$ [Eqs. (A9) and (A10)] over the g-factor fluctuations, we can use the following approximation: $S^{\infty}\approx(S^{\infty})_{\beta=\beta_0}$. For $S_1(t)$, we obtain the approximate expression

$$S_{1X}(t) = S_{0X}e^{-(\tau^2/4)(1+2\Delta_\beta^2)}\left\{\left[1-\frac{1}{2\beta_0^2}\left(1-\frac{I_2(\beta_0,\tau)}{2\beta_0}\right)\right]\cos(\beta_0\tau) - \frac{\tau}{2\beta_0}\left(1-\frac{I_1(\beta_0,\tau)}{4\beta_0}\right)\sin(\beta_0\tau)\right\} - S_{0X}e^{-(\tau^2/4)}\frac{e^{-\beta_0^2}I_2(0,\tau)}{4\beta_0^3},$$

$$S_{1Y}(t) = -S_{0X}e^{-(\tau^2/4)(1+2\Delta_\beta^2)}\left\{\left(1-\frac{1}{2\beta_0^2}\right)\sin(\beta_0\tau) + \frac{\tau}{2\beta_0}\cos(\beta_0\tau)\right\},$$

$$S_{1Z}(t) = \frac{S_{0Z}}{\beta_0^2}e^{-(\tau^2/4)(1+2\Delta_\beta^2)}\left\{\left(1-\frac{I_2(\beta_0,\tau)}{2\beta_0}\right)\cos(\beta_0\tau) - \frac{\tau}{2\beta_0}\frac{I_1(\beta_0,\tau)}{2}\sin(\beta_0\tau)\right\} + S_{0Z}e^{-(\tau^2/4)}\frac{e^{-\beta_0^2}I_2(0,\tau)}{2\beta_0^3}. \tag{A22}$$

The calculation frame $(OXYZ)$ is obtained from the initial one $(Oxyz)$ by performing two rotations. One with Oy axis with an angle η': $R_{Oy}(\eta')(Oxyz)=(Ox'y'z')$ such that $Oz' \| \mathbf{\Omega}_{ext}$. The second with Oz' axis and angle ϕ: $R_{Oy}(\phi)\times(Ox'y'z')=(OXYZ)$ such that the plane (XOZ) contains $\mathbf{S}_0$. We can, thus, obtain the general expression of the electron-spin evolution in the frame $(Oxyz)$ by

$$\begin{pmatrix} S_x(t) \\ S_y(t) \\ S_z(t) \end{pmatrix} = \begin{pmatrix} \cos\eta'\cos\phi & -\cos\eta'\sin\phi & \sin\eta' \\ \sin\phi & \cos\phi & 0 \\ -\sin\eta'\cos\phi & \sin\eta'\sin\phi & \cos\eta' \end{pmatrix} \times \begin{pmatrix} S_X(t) \\ S_Y(t) \\ S_Z(t) \end{pmatrix}.$$

For a pure transverse magnetic field, $\eta=\eta'=\pi/2$ and $\phi=0$, so the transformation takes the simple form

$$\begin{pmatrix} S_x(t) \\ S_y(t) \\ S_z(t) \end{pmatrix} = \begin{pmatrix} S_Z(t) \\ S_Y(t) \\ -S_X(t) \end{pmatrix}. \tag{A23}$$

In addition, as here $\mathbf{S}_0=S_{0z}\mathbf{e}_z$, we have $S_x(t)=S_y(t)=0$ and $S_z(t)=-S_X(t)$. Some examples are given in Figs. 1, 4, and 5.

*Electronic address: amand@insa-toulouse.fr

[1] D. Awschalom, D. Loss, and N. Samarth, *Semiconductor Spintronics and Quantum Computation*, NanoScience and Technology (Springer, Berlin, 2002).

[2] D. P. DiVincenzo, Science **270**, 255 (1995).

[3] A. Imamoglu, D. D. Awschalom, G. Burkard, D. P. DiVincenzo, D. Loss, M. Sherwin, and A. Small, Phys. Rev. Lett. **83**, 4204 (1999).

[4] I. Zutic, J. Fabian, and S. D. Sarma, Rev. Mod. Phys. **76**, 323 (2004).

[5] D. P. DiVincenzo, G. Burkard, D. Loss, and E. V. Sukhorukov, *Quantum Mesoscopic Phenomena and Mesoscopic Devices in Microelectronics*, edited by I. O. Kulik and R. Elliatioglu (NATO Advanced Study Institute, Turkey, 1999).

[6] M. Kroutvar, Y. Ducommun, D. Heiss, M. Bichler, D. Schuh, G. Abstreiter, and J. J. Finley, Nature (London) **432**, 81 (2004).

[7] J. M. Elzerman, R. Hanson, L. H. W. van Beveren, B. Witkamp, L. M. K. Vandersypen, and L. P. Kouwenhoven, Nature (London) **430**, 431 (2004).

[8] F. Meier and B. Zakharchenya, *Optical Orientation, Modern Problems in Condensed Matter Sciences* Vol 8 (North-Holland, Amsterdam, 1984).

[9] V. N. Golovach, A. Khaetskii, and D. Loss, Phys. Rev. Lett. **93**, 016601 (2004).

[10] J. R. Petta, A. C. Johnson, J. M. Taylor, E. A. Laird, A. Yacoby, M. D. Lukin, C. M. Marcus, M. P. Hanson, and A. C. Gossard, Science **309**, 2180 (2005).

[11] A. Greilich, D. R. Yakovlev, A. Shabaev, A. L. Efros, I. A. Yugova, R. Oulton, V. Stavarache, D. Reuter, A. Wieck, and M. Bayer, Science **313**, 341 (2006).

[12] A. S. Lenihan, M. V. Gurudev Dutt, D. G. Steel, S. Ghosh, and P. K. Bhattacharya, Phys. Rev. Lett. **88**, 223601 (2002).

[13] A. I. Tartakovskii, J. Cahill, M. N. Makhonin, D. M. Whittaker, J.-P. R. Wells, A. M. Fox, D. J. Mowbray, M. S. Skolnick, K. M. Groom, M. J. Steer, and M. Hopkinson, Phys. Rev. Lett. **93**, 057401 (2004).

[14] M. Sénès, B. Urbaszek, X. Marie, T. Amand, J. Tribollet, F. Bernardot, C. Testelin, M. Chamarro, and J.-M. Gérard, Phys. Rev. B **71**, 115334 (2005).

[15] S. Laurent, M. Senes, O. Krebs, V. K. Kalevich, B. Urbaszek, X. Marie, T. Amand, and P. Voisin, Phys. Rev. B **73**, 235302 (2006).

[16] I. A. Merkulov, A. L. Efros, and M. Rosen, Phys. Rev. B **65**, 205309 (2002).

[17] A. V. Khaetskii, D. Loss, and L. Glazman, Phys. Rev. Lett. **88**, 186802 (2002).

[18] Y. G. Semenov and K. W. Kim, Phys. Rev. B **67**, 073301 (2003).

[19] I. A. Akimov, D. H. Feng, and F. Henneberger, Phys. Rev. Lett. **97**, 056602 (2006).

[20] P.-F. Braun, X. Marie, L. Lombez, B. Urbaszek, T. Amand, P. Renucci, V. K. Kalevich, K. V. Kavokin, O. Krebs, P. Voisin *et al.*, Phys. Rev. Lett. **94**, 116601 (2005).

[21] A. Greilich, R. Oulton, E. A. Zhukov, I. A. Yugova, D. R. Yakovlev, M. Bayer, A. Shabaev, A. L. Efros, I. A. Merkulov, V. Stavarache *et al.*, Phys. Rev. Lett. **96**, 227401 (2006).

[22] M. Bayer, A. Kuther, A. Forchel, A. Gorbunov, V. B. Timofeev, F. Schafer, J. P. Reithmaier, T. L. Reinecke, and S. N. Walck, Phys. Rev. Lett. **82**, 1748 (1999).

[23] B. Eble, O. Krebs, A. Lemaître, K. Kowalik, A. Kudelski, P. Voisin, B. Urbaszek, X. Marie, and T. Amand, Phys. Rev. B **74**,

081306(R) (2006).
[24] S. Cortez, O. Krebs, S. Laurent, M. Senes, X. Marie, P. Voisin, R. Ferreira, G. Bastard, J.-M. Gérard, and T. Amand, Phys. Rev. Lett. **89**, 207401 (2002).
[25] T. C. Damen, L. Vina, J. E. Cunningham, J. Shah, and L. J. Sham, Phys. Rev. Lett. **67**, 3432 (1991).
[26] S. E. Economou, R.-B. Liu, L. J. Sham, and D. G. Steel, Phys. Rev. B **71**, 195327 (2005).
[27] M. V. Gurudev Dutt, J. Cheng, B. Li, X. Xu, X. Li, P. R. Berman, D. G. Steel, A. S. Bracker, D. Gammon, S. E. Economou, R. B. Liu, and L. J. Sham, Phys. Rev. Lett. **94**, 227403 (2005).
[28] A. Abragam, *Principles of Nuclear Magnetism* (Oxford Science, New York, 1961).
[29] E. Gryncharova *et al.*, Sov. Phys. Semicond. **11**, 997 (1977).
[30] M. Paillard, X. Marie, P. Renucci, T. Amand, A. Jbeli, and J. M. Gerard, Phys. Rev. Lett. **86**, 1634 (2001).
[31] A. Greilich, R. Oulton, S. Y. Verbin, R. Cherbunin, T. Auer, D. Yakovlev, M. Bayer, V. Stavarache, D. Reuter, and A. Wieck, arXiv:cond-mat/0505446 (unpublished).
[32] E. Ivchenko, A. Kiselev, and M. Willander, Solid State Commun. **102**, 375 (1997).
[33] X. Marie, P. Le Jeune, T. Amand, M. Brousseau, J. Barrau, M. Paillard, and R. Planel, Phys. Rev. Lett. **79**, 3222 (1997).
[34] A. Malinowski, D. J. Guerrier, N. J. Traynor, and R. T. Harley, Phys. Rev. B **60**, 7728 (1999).
[35] G. Hendrofer and J. Schneider, Semicond. Sci. Technol. **6**, 595 (1991).
[36] M. Bayer, A. Kuther, F. Schafer, J. P. Reithmaier, and A. Forchel, Phys. Rev. B **60**, R8481 (1999).
[37] A. P. Heberle, J. J. Baumberg, and K. Kohler, Phys. Rev. Lett. **75**, 2598 (1995).
[38] T. Amand, X. Marie, P. Le Jeune, M. Brousseau, D. Robart, J. Barrau, and R. Planel, Phys. Rev. Lett. **78**, 1355 (1997).
[39] P.-F. Braun, B. Urbaszek, T. Amand, X. Marie, O. Krebs, B. Eble, A. Lemaître, and P. Voisin, Phys. Rev. B **74**, 245306 (2006).
[40] D. Paget, G. Lampel, B. Sapoval, and V. I. Safarov, Phys. Rev. B **15**, 5780 (1977).
[41] B. Patton, W. Langbein, and U. Woggon, Phys. Rev. B **68**, 125316 (2003).
[42] T. Flissikowski, A. Hundt, M. Lowisch, M. Rabe, and F. Henneberger, Phys. Rev. Lett. **86**, 3172 (2001).
[43] W. Langbein, P. Borri, U. Woggon, V. Stavarache, D. Reuter, and A. D. Wieck, Phys. Rev. B **69**, 161301(R) (2004).
[44] If $\mathbf{B}_{ext}$ has a longitudinal component, dynamical polarization of the nuclei may occur. In that case, the calculation can be performed by adding some static contribution to $\mathbf{\Omega}_{ext}$, corresponding to the ensemble average of the nuclear precession vector (Ref. 40).
[45] We consider here that the lifetime of the radiative transition is the same for X^0, X^+, or X^{2+}, and that the electron-hole anisotropic exchange interaction is comparable for X^0 and X^{2+}.